

An Examination of Applying Shunted Piezoelectrics to Reduce Aeroelastic Response

Anna-Maria Rivas McGowan*

NASA Langley Research Center, MS 340, Hampton, VA 23681-2199

ABSTRACT

Several analytical and experimental studies clearly demonstrate that piezoelectric materials (piezoelectrics) can be used as actuators to actively control vibratory response, including aeroelastic response. However, two important issues in using piezoelectrics as actuators for active control are: 1) the potentially large amount of power required to operate the actuators, and 2) the complexities involved with active control (added hardware, control law design, and implementation). Active or passive damping augmentation using shunted piezoelectrics may provide a viable alternative. This approach requires only simple electrical circuitry and very little or no electrical power. The current study examines the feasibility of using shunted piezoelectrics to reduce aeroelastic response using a typical-section representation of a wing and piezoelectrics shunted with a parallel resistor and inductor. The aeroelastic analysis shows that shunted piezoelectrics can effectively reduce aeroelastic response below flutter and may provide a simple, low-power method of subcritical aeroelastic control.

1. INTRODUCTION

Over the last decade, smart material-based actuation systems (or “smart devices”) have been studied as potential alternatives to the use of conventional control mechanisms for controlling aeroelastic response. The use of smart devices introduces a unique facet in controlling dynamic aeroelastic response: the use of structural forces, as opposed to aerodynamic forces, for control. The ability to effectively and efficiently control structural response via internal structural forces or dampers may allow aircraft designers to take advantage of the inherent flexibility in air vehicles to create more efficient structural designs that may also improve flight performance. Ultimately, the use of smart devices can be used in combination with conventional aerodynamic control surfaces to allow for many new active and/or passive aeroelastic control approaches.

Due to their 20 KHz bandwidth and effectiveness in strain actuation, piezoelectric materials used as actuators have been the smart device of choice for aeroelastic control applications. Numerous studies have shown that piezoelectric actuators can be used to control structural and aeroelastic response. References 1 - 3 provide comprehensive overviews of work in aeroelastic control using piezoelectric and other smart materials-based actuators. In particular, the research described in references 4, 5, and 6 were instrumental not only in demonstrating the benefits of using piezoelectric actuators for active aeroelastic control, but also in addressing some of the many realistic issues associated with applying piezoelectric actuators to large and full-scale structures. Two critical issues in using piezoelectrics as actuators for active control are the potentially large amount of power required to operate the actuators and the complexities of active control. For example, reference 7 states that the power required to control a structure using piezoelectric patch actuators is a function of the voltage squared. Since high voltages (i.e., 200 volts) and a large number of piezoelectric actuators are typically required to control vibration on large structures, the amount of power required can be considerable. Secondly, active control approaches using smart or conventional actuators generally have the additional complexities of a control law, substantial additional hardware, and possible, unplanned instabilities caused by the control law.

One potential alternative is damping augmentation using shunted piezoelectrics. This approach allows for active or passive damping augmentation, yet cannot cause instability. Furthermore, shunted piezoelectrics use little to no power and are simple to apply; the only necessary hardware is the piezoelectrics themselves and simple electric circuitry using resistors and inductors. The present research examines the feasibility of using shunted piezoelectrics (shunted by a parallel resistor and inductor) to reduce aeroelastic response at speeds below flutter. A typical-section

representation of a wing is used and the shunted piezoelectrics are represented as a damped vibration absorber placed on the elastic axis of the wing. The analytical approach taken in the current work is an extrapolation of existing analytical methods, which primarily focus on application of shunted piezoelectrics to simple beams and plates. As such, following background information, this report first documents the application of shunted piezoelectrics to a simple one-dimensional structure and discusses the constraints and assumptions made in the existing analytical methods. Following this, the aeroelastic equations of motion are derived for a two degree-of-freedom typical wing section with shunted piezoelectrics placed on the elastic axis. Using this aeroelastic model, the response of the typical section to external forcing functions is shown at several airspeeds. Observations as to the response reduction are provided and the potential impact on future air vehicle designs are discussed. All derivations in the current document are summarized to save space. A more detailed analysis can be found in reference 8.

2. BACKGROUND

A number of studies have been conducted on the behavior of electric circuits used for shunting. 9-24 In particular, reference 9 presents a derivation of the effective mechanical impedance for a piezoelectric shunted by an arbitrary circuit. This work focused on resistive and series resistor, inductor, and capacitor (RLC) circuits and forms the basis for the present work. In addition, references 18 and 19 discuss the parallel RLC shunt circuit and follow the methodology of reference 9 to develop an associated analytical model; these references are also used for the current work. Furthermore, in reference 20, Wu shows experimental results using parallel RLC circuits to add damping to multiple modes.

The foregoing research efforts clearly demonstrate the effectiveness of using shunted piezoelectrics to reduce vibration amplitudes. Reference 21 presents a good discussion of the some of the practical limitations and some analytical models. In addition, reference 22 provides a comparison of the use of piezoelectrics for damping augmentation versus constrained layer damping. Application of shunted piezoelectrics to a variety of areas has been considered (although not all results have been published) including vibration suppression and acoustic damping on flight vehicles, space structures²³, and machinery. In some cases, simple scale-model experiments have been conducted. Although many researchers have demonstrated the viability of shunted piezoelectrics in laboratory experiments with much success, commercial or full-scale demonstrations are limited. As mentioned earlier, the current work seeks to analytically examine the feasibility of using piezoelectrics, shunted via a parallel resistor and inductor, to reduce aeroelastic response. The analysis allows numerous observations and conclusions; however, final application in an aircraft wing or tail will certainly require considerable additional research and, of course, experimental studies.

A parallel RLC shunt circuit was chosen for the current study because it is much more effective than a resistive shunt circuit and it is easier to tune than a series RLC shunt circuit. In practice, use of a parallel or series RLC shunt circuits usually requires a simulated inductor. Without the simulated inductor, large and heavy inductors would be required to shunt the average-sized piezoelectric.¹⁸ Reference 12 shows that lightweight, compact, simulated inductors can be created using operational amplifiers and resistors. Furthermore, use of a simulated inductor enables active shunting wherein the shunt circuit is actively “tuned” as the host structure changes. More discussion of tuning the shunt circuit is provided subsequently. The analysis for the current feasibility study begins with the piezoelectric constitutive relations, which are augmented to include the effects of the parallel RLC shunt circuit.

2.1 Piezoelectric constitutive relations

The piezoelectric constitutive equations, assuming linearity and uniaxial loading are well documented. Addition of the shunt circuit is accomplished by augmenting the electrical impedance in the constitutive equations with that of a parallel RLC electrical circuit. For the current study, conventional, one-way electro-mechanical coupling was employed such that the coupled (open-circuit) compliance with the addition of the shunt circuit is:

$$s_{11}^{OC,SH}(\tilde{s}) = s_{11}^{OC,PZT} \left[\frac{\tilde{s}^2 RLC^S + \tilde{s}L + R}{(1 - k_{31}^2)(\tilde{s}L + R) + \tilde{s}^2 RLC^S} \right] \quad (1)$$

The electro-mechanical coupling coefficient, k_{31} , is used for simplicity where: $k_{ij} = d_{ij} / \sqrt{s_{ij}^{SC} \epsilon_i^T}$ and ϵ is the dielectric constant.²⁵ In equation 1, the follow definitions were used: \tilde{s} is the Laplace variable, C^S is capacitance at constant strain, R is resistance, and L is inductance. The compliance shown in equation 1 will be used to represent the compliance of the shunted piezoelectric in the subsequent equations of motion. Recall that uniaxial loading of the piezoelectric was assumed; as such, equation 1 only reflects the compliance in extension (the “1” direction in Figure 1).

3. SHUNTED PIEZOELECTRICS APPLIED TO A GENERIC HOST STRUCTURE

3.1 Description of the analytical model

Application of shunted piezoelectrics to a generic host structure is considered to form a basis for the more complex aeroelastic studies that will be examined next. Moreover, application to a generic structure allows for clear examination of the general characteristics of shunted piezoelectrics and examination of the implications of the assumptions and constraints employed in the current analytical methods. The analytical methods presented in references 9 and 18 were primarily followed with a few noted exceptions.

The equation of motion for a generic host structure with a surface-bonded piezoelectric, as shown in Figure 2, is developed based on the following assumptions:

- 1) The thickness and length of the piezoelectric are small compared to that of the host structure.
- 2) The inertial effects of the piezoelectric are negligible.
- 3) The piezoelectric is poled in the “3” direction and only displacement in the “1” direction is considered. This assumption is consistent with the assumption of uniaxial loading on the piezoelectric.
- 4) An external shunt circuit consisting of a resistor and inductor connected in parallel is attached to the electrodes of the piezoelectric creating a parallel resistor-inductor-capacitor electric circuit.
- 5) The “1” direction of the piezoelectric is perpendicular to the bending node lines of the host structure, such that the shunted piezoelectric acts primarily to reducing bending response. Thus, torsion vibration modes are largely unaffected by the damping characteristics of the shunted piezoelectric and are not represented in the equation of motion.
- 6) Damping in the host structure is negligible.

Considering the bending degree of freedom only, the equation of motion in terms of Laplace transforms and the mechanical impedance of the host structure with shunted piezoelectrics is:

$$Z_{SYS}^{mech}(\tilde{s}) = m_{STR} \tilde{s} + \frac{K_{STR}}{\tilde{s}} + Z_{PZT}^{mech}(\tilde{s}) \quad (2)$$

The mass of the piezoelectric can easily be included in the equations of motion by adding the term $m_{PZT} \tilde{s}$. However, as mentioned in the assumptions above, this term is normally not necessary since the inertial characteristics of the piezoelectric are negligible for most applications. The mechanical impedance of a shunted piezoelectric can be modeled as:

$$Z_{PZT}^{mech}(\tilde{s}) = \frac{K_{PZT}(\tilde{s})}{\tilde{s}} = \frac{T_1(\tilde{s}) \cdot A_1}{\tilde{s} \cdot S_1(\tilde{s}) \cdot L_1} = \frac{A_1}{\tilde{s} \cdot L_1 \cdot s_{11}^{OC,SH}(\tilde{s})} \quad (3)$$

where the extensional stiffness of the piezoelectric in the “1” direction is used (see Figure 1). There are a few important observations concerning the use of the extensional stiffness of the piezoelectric. Though the extensional stiffness of the piezoelectric is considerable (piezoelectric materials have a Young’s Modulus on the order of aluminum), that stiffness does not significantly affect the response of the host structure primarily because the piezoelectrics are short and thin compared to the host structure. Thus, the effect of this stiffness on the response of

the host structure is negligible unless numerous piezoelectrics are used. In addition, it is important to remember that the above equations were developed assuming a simple, lumped-parameter system. To obtain the best results using this idealization, use of experimentally-measured values for the natural frequency of the host structure are required. Alternatively, a more rigorous definition of piezoelectric stiffness can be used, an example of which is derived in reference 26.

Referring again to equation 3, the open-circuit compliance of the shunted piezoelectric (from equation 1) must be incorporated. Thus, including the mechanical impedance of the shunted piezoelectric into the equation of motion (equation 2) yields:

$$Z_{SYS}^{mech}(\tilde{s}) = m_{STR} \tilde{s} + \frac{(K_{STR} + K_{PZT}^{SC})}{\tilde{s}} + \left(\frac{K_{PZT}^{OC}}{\tilde{s}} \right) \frac{k_{31}^2 (\tilde{s} R L C^S)}{(\tilde{s}^2 R L C^S + \tilde{s} L + R)} \quad (4)$$

where: $K_{PZT}^{SC} = A_1 / (L_1 s_{11}^{SC})$ and $K_{PZT}^{OC} = A_1 / (L_1 s_{11}^{OC})$ are the short-circuit and open-circuit stiffnesses of the piezoelectric, respectively. Note that, K_{PZT}^{SC} is the stiffness of the piezoelectric without any external electrical stimulus (i.e., shunt circuit or control law input). Then, it follows that the normalized response of the host structure response is:

$$\frac{X(\tilde{s})}{X_{st}(\tilde{s})} = \frac{-(G^2 - \Omega^2) + i2\zeta G}{-\left[\bar{K}_{31}^2 G^2 - (G^2 - 1)(G^2 - \Omega^2) \right] - i2\zeta G(G^2 - 1)} \quad (5)$$

The following dimensional and nondimensional terms are used for simplification: $X_{st}(\tilde{s}) = F(\tilde{s}) / K_{STR}$;

$\omega_{SC}^2 = (K_{STR} + K_{PZT}^{SC}) / m_{STR}$; $\omega_{OC}^2 = (K_{STR} + K_{PZT}^{OC}) / m_{STR}$; $\bar{K}_{31}^2 = (\omega_{OC}^2 - \omega_{SC}^2) / \omega_{SC}^2$ (which is the generalized electro-mechanical coupling coefficient); $\omega_E^2 = 1 / (L C^S)$; $\zeta = 1 / (2 R C^S \omega_{SC})$; $\Omega^2 = \omega_E^2 / \omega_{SC}^2$; and, $G = \omega / \omega_{SC}$. Furthermore, based on the above terms, the inductance in the shunt circuit is defined as: $L = 1 / (\omega_{SC}^2 \Omega^2 C^S)$. Likewise, the resistance is defined as: $R = 1 / (2 \omega_{SC} \zeta C^S)$.

Several important observations can be made regarding the above nondimensional parameters. First, the short-circuit natural frequency, ω_{SC} , is the natural frequency of the system without any external electric stimulus. Thus, for the model considered, ω_{SC} represents the bending natural frequency of the structure including the stiffness of the piezoelectric but not the effects of the shunt circuit. Second, the generalized electro-mechanical coupling coefficient, \bar{K}_{31} , is the ratio of the short-circuit modal stiffness of the piezoelectric to the total system modal stiffness. As such, \bar{K}_{31} is proportional to the fraction of system modal strain energy that is converted to electric energy by the open-circuit piezoelectric, and thus, is a measure of the shunted piezoelectric's influence on the system.⁹ Clearly, this influence is ultimately determined by how well the piezoelectric is bonded to the host structure. More accurate representation of the characteristics of the adhesive used to bond the piezoelectrics may require a higher fidelity representation of this coupling coefficient. However, experimental results show that the above representation is typically suitable.¹⁹ The final nondimensional parameter to note is the damping ratio, ζ . The definition for ζ used herein differs from that currently published in the literature. The damping ratio used above is the mechanical analog of the damping ratio of a parallel RLC electric circuit. Previous references (e.g., 9, 13, 16, 18, 19, and 20) use $\zeta = R C^S \omega_{SC}$, which is appropriate for a series resistor-inductor-capacitor shunt circuit but not for a parallel circuit such as the one used in the current work. Note that Wu (in references 18 and 19) also uses a parallel circuit and obtains the same function for normalized amplitude as shown in equation 5 using different terminology. In particular, he defines damping ratio as $\zeta = R C^S \omega_{SC}$. Either definition of damping ratio (Wu's^{18,19} or the one used herein) is acceptable as long as it is used consistently. Quantitative comparisons with results from previous derivations will be shown in the next section.

3.2 Failure scenarios

Equation 5 can be used to determine the response of the host structure for various values of resistance, inductance and capacitance (piezoelectrics). As will be discussed in the next section, accurately selecting the shunt circuit

parameters is critical to obtaining optimal response reduction. Before optimum conditions of the shunt circuit are examined, it is informative to examine the response of the host structure for extreme conditions of the shunt circuit. One such condition is complete failure, or a disconnection, of the shunt electric components (the resistor and inductor). In this case, the piezoelectric merely adds a small amount of stiffness to the host structure and dissipates a little strain energy. Though the piezoelectrics considered herein are assumed to be massless, inclusion of the mass of the piezoelectrics typically has negligible effects on the dynamic response of the host structure.

The other extreme condition is a shunt circuit with values of resistance and inductance that are extremely different from the values needed for optimum response reduction. This condition raises the question: Can the addition of the shunt circuit to the piezoelectric cause an increase in the response of the host structure, or even cause an instability in the structure? Two characteristics of the shunt circuit prevent this from occurring: 1) the shunt circuit has no external energy source, such as a voltage or current source; and 2) the resistor in the circuit will always dissipate energy. Thus, use of a shunted piezoelectric will be a fail-safe system for the vast majority of applications. The only way in which adding shunted piezoelectrics (that are not also being used as actuators) to a structure can worsen the dynamic response of the structure is if the weight of the piezoelectrics is considerable, and if the piezoelectrics are placed far from the structure's center of gravity. In this case, the piezoelectrics (regardless of the tuning of or the existence of the shunt circuit) will act as an unbalanced mass on the structure. Practically speaking, if the weight of the piezoelectrics used is significant enough to cause this type of complication, then piezoelectrics are most likely not to be the best choice for reducing structural response. However, as mentioned above, a condition exists, between the two extremes discussed, that yields optimal response reduction of the host structure.

3.3 Damped vibration absorber analogy

Adjusting or tuning the shunt circuit to obtain optimal response reduction is greatly simplified by using the "tuning" techniques developed for damped vibration absorbers. These techniques apply because shunted piezoelectrics can essentially be modeled as damped vibration absorbers (DVA). This analogy becomes clear by examining the nondimensional or normalized response of a lumped mass system with an attached damped vibration absorber as shown in Figure 3 and described using equation 6. The DVA is represented by mass, m_2 , stiffness, k_2 , and damping, c_2 ; the host structure is represented by mass, m_1 , and stiffness, k_1 .

The nondimensional response of the system shown in Figure 3 is:

$$\frac{x_1(\tilde{s})}{x_{st}(\tilde{s})} = \frac{x_1(\tilde{s})}{F_1(\tilde{s})/k_1} = \frac{-(G^2 - \Omega^2) + i2\zeta G}{- [M\Omega^2 G^2 - (G^2 - 1)(G^2 - \Omega^2)] - i2\zeta G(G^2 - 1 + MG^2)} \quad (6)$$

where: $\omega_1^2 = \frac{k_1}{m_1}$, $\omega_2^2 = \frac{k_2}{m_2}$, $\Omega^2 = \frac{\omega_2^2}{\omega_1^2}$, $G^2 = \frac{\omega^2}{\omega_1^2}$, $M = \frac{m_2}{m_1}$, $c_c = 2m_2\omega_1$, $\zeta = \frac{c_2}{c_c}$. Note that Italics are used to

describe the damped vibration absorber system to distinguish it from the other equations used in this report. Examination of equation 6 reveals many similarities to equation 5. The only two differences in the equations are: 1) the squared generalized electro-mechanical coupling coefficient, \bar{K}_{31}^2 , of equation 5 is analogous to the $M\Omega^2$ term in equation 6; and 2) equation 6 contains the term $i2\zeta MG^3$, which does not exist in equation 5, and no simple analog is obvious. However, the overall behavior of the normalized amplitude in equation 6 is still maintained when the term $i2\zeta MG^3$ is removed. Thus, the normalized response of a host structure with attached shunted piezoelectrics (defined in equation 5) is very similar to the normalized response of a simple, lumped-parameter spring mass with an attached damped vibration absorber (defined in equation 6).

As with any analogy, however, there are limitations to the use of the above mentioned analogy of a damped vibration absorber to shunted piezoelectrics. For very large and very small damping ratios, ζ , the analogy between the damped vibration absorber and shunted piezoelectrics is not appropriate because neither condition can be realistically attained by the shunted piezoelectric. At these conditions, the term $i2\zeta MG^3$ becomes significant in the damped vibration

absorber. Very large damping ratios (i.e., ζ approaching infinity) simulate the two masses in Figure 3 being locked together such that their relative displacement is zero and thus, no work is done by the damping force. For the shunted piezoelectric, this condition equates to an “infinite” stiffness in the piezoelectric such there is no displacement in the piezoelectric. The above case of an “infinite” stiffness piezoelectric is not realistic. On the other hand, very small damping ratios signify that the damping force is near zero and very little, if any, energy dissipation takes place. For some conditions of m_2 and k_2 and with $\zeta_2 = 0$ in the damped vibration absorber, this means that the presence of the damped vibration absorber can further amplify the motion of the host structure, particularly if the host structure has damping. Since the piezoelectric material has inherent damping, the piezoelectric will always dissipate some energy from the motion of the host structure regardless of the existence of, or the components in, the shunt circuit. Furthermore, since the shunt circuit described herein can not supply voltage to the piezoelectric (and thus, create an actuator) and the resistor in the shunt circuit always dissipates some energy from the piezoelectric, the case of zero damping is unrealistic for a shunted piezoelectric. Moreover, cases of near zero damping ratios must be carefully examined to ensure realism. Also, note that since the shunted piezoelectrics were considered massless for the current study, the above scenario is precluded for the results herein.

3.4 Tuning the shunt circuit

As with the shunted piezoelectric circuit, appropriate tuning is required for the damped vibration absorber to reduce the response of the host structure most effectively. Tuning requires adjusting the parameters Ω and ζ for both the damped vibration absorber and the shunted piezoelectric circuit. The same methodology used to tune a damped vibration absorber can be applied to tune a shunted piezoelectric circuit since the two systems perform similarly. This tuning methodology is described in several references (see e.g., references 27, 28, and 29). An abbreviated summary (shown below) of one method to tune a damped vibration absorber (DVA) is applied to tuning the shunt circuit.

Tuning is accomplished using equation 5 in combination with Figure 4. Figure 4 depicts nondimensional response of the host structure, with shunted piezoelectrics as described in equation 5, plotted using several values of damping ratio and an untuned value of frequency ratio, $\Omega=0.9466$. The first step in tuning is to find the optimal frequency ratio Ω_{opt} . Use of Ω_{opt} ensures the electrical natural frequency of the shunt circuit is tuned to create an electrical antiresonance (infinite electrical impedance) at the frequency of the structural mode of interest. Graphically, using Ω_{opt} equates to making the two “peaks” of the response of the host structure with shunted piezoelectrics the same height (see Figure 4).

Finding Ω_{opt} begins with identifying the nondimensional frequencies, G_1 and G_2 , corresponding to points A and B in Figure 4. Note that all curves pass through points A and B regardless of the value of damping ratio. G_1 and G_2 are defined: $G_{1,2}^2 = 1 \pm \bar{K}_{31}/\sqrt{2}$. The second step is to force the nondimensional amplitudes at points A and B in Figure 4 to be equal and solve for the optimal (tuned) frequency ratio Ω_{opt} :

$$\Omega_{opt}^2 = 1 - \bar{K}_{31}^2/2 \quad (7)$$

Using the above frequency ratio, the inductance for the shunt circuit can be obtained. The optimal inductance is:

$$L_{opt} = 1/(\omega_{SC}^2 \Omega_{opt}^2 C^S) \quad (8)$$

Next, the optimal damping ratio must be found; this enables optimum energy dissipation through the resistor at the optimal frequency. Thus, optimal damping ratio is a function of optimal frequency ratio. Graphically, use of the optimal damping ratio ensures the two, level peaks of the response are at their lowest value. Thus, to find ζ_{opt} , the optimal frequency, Ω_{opt} , is used and the slope at points A or B is set to zero. Optimal damping ratio can then be written as:

$$\zeta_{opt} = \frac{1}{4\sqrt{1 \pm \frac{\bar{K}_{31}}{\sqrt{2}}}} \left[\left(2 - \frac{\bar{K}_{31}^2}{2} - 2 \left(1 \pm \frac{\bar{K}_{31}}{\sqrt{2}} \right) \right) \mp \bar{K}_{31} \sqrt{2 - \frac{5}{4} \bar{K}_{31}^2 + 2 \left(1 \pm \frac{\bar{K}_{31}}{\sqrt{2}} \right)} \right] \quad (9)$$

This expression for optimal damping ratio differs from that shown in previous references for two reasons: 1) damping ratio is defined differently in the current text, as mentioned earlier; and 2) the procedure used in the present work to find optimal damping ratio differs from previous references. For example, using $\zeta = RC^S\omega_{SC}$, Wu defines optimal damping ratio as $\zeta_{opt} = 1/(\sqrt{2\bar{K}_{31}})$ in reference 18. A numerical example will be used to examine the accuracy of both definitions subsequently. Note that the magnitude of the damping ratio shown in equation 9 can be used to obtain the resistance value for the shunt circuit. The optimal (tuned) resistance in the shunt electric circuit is:

$$R_{opt} = 1/(2\omega_{SC}C^S|\zeta_{opt}|) \quad (10)$$

Hence, using equations 8 and 10, the inductance and resistance of the shunt circuit can be tuned for optimal response reduction for a given value of capacitance in the piezoelectric, C^S . For active control using the shunt circuit, the inductance and resistance would be actively adjusted as the host structure changes. For passive control, the shunt circuit would be tuned for the condition of interest and the resistance and inductance would not be updated as the host structure changes.

3.5 Analytical validation and limitations of the tuning methodology

The validity of the derivations for optimal frequency and damping ratio can be determined by using a simple example. First, the peak nondimensional amplitude of the host structure's response at the optimum condition is at frequencies, G_1 and G_2 , which are the locations of points A and B. To find this amplitude, the simplest form of the equation for nondimensional amplitude may be used since the amplitude at these frequencies is independent of damping: $\frac{X(\tilde{s})}{X_{st}(\tilde{s})}\Big|_{\zeta=\infty} = \frac{1}{G^2 - 1}$. Thus, the peak nondimensional amplitude at optimum response reduction is:

$$\frac{X(\tilde{s})}{X_{st}(\tilde{s})}\Big|_{G_1} = \frac{\sqrt{2}}{\bar{K}_{31}} \quad (11)$$

Note that equation 11 was obtained without using any tuning parameters and thus can be used to check the validity of the results using the tuning parameters.

As an example, assume a host structure with shunted piezoelectrics where $\bar{K}_{31} = 0.12$, which is a typical value. The response of this host structure at untuned values is shown in Figure 4. Figure 4 shows the response of the host structure using the optimal frequency ratio, as calculated using equation 7, and using the magnitude of the optimal damping ratio, as calculated using equation 9. The peak nondimensional amplitude of the response using the calculated tuning parameters is: 11.79. Using equation 11, the peak response at optimum response reduction is: $(X(\tilde{s})/X_{st}(\tilde{s}))\Big|_{G_1} = 11.79$ which indicates the accuracy of the derivations herein.

As a comparison, the definitions used in current literature can also be examined. The optimum frequency ratio used herein is the same as that in current literature; however, the definition of damping ratio and the derivation of optimal damping ratio differs. Using the definition for damping ratio as specified in current literature and using the corresponding optimum damping ratio defined as $\zeta_{opt} = 1/(\sqrt{2\bar{K}_{31}})$ in reference 18, yields a peak nondimensional amplitude of 12.19 for the same example. Thus, both definitions of damping ratio can be used to obtain the optimum values; however, for the simple lumped-parameter system considered, a more accurate calculation for optimum tuning parameters is possible using the derivations developed herein.

It is crucial to recall that the preceding tuning methodology was developed following the methodology used to tune a damped vibration absorber (shown in Figure 3), where the host structure (represented by m_I and k_I) does not have damping ($c_I = 0$). When the host structure has damping, two important characteristics of the response become apparent. First, with damping in the host structure, it is very difficult to derive closed-form solutions for Ω_{opt} and

ζ_{opt} as was done previously, primarily because two unique points such as A and B no longer exist. However, as mentioned in reference 13, the above tuning techniques may still be used reliably for structures that have small damping. These tuning techniques can be used by either neglecting the damping in the host structure and solving the above equations or by accounting for the damping using an iterative computational procedure. Both techniques should yield similar answers for Ω_{opt} and ζ_{opt} because the tuning parameters are not highly a function of the damping that exists in the host structure. Reference 30 provides an alternative technique for tuning a system that has small damping.

The second important characteristic of the response when the host structure has damping is that the effectiveness of the shunted piezoelectric (and likewise the damped vibration absorber) is strongly dependent on the damping of the host structure. Increased damping in the host structures results in decreased effectiveness of the shunted piezoelectric because the shunted piezoelectric is primarily adding damping to the host structure. The larger the damping inherent in the system, the less the percentage of total system damping the shunted piezoelectric can add.

In the next section, a two-degree-of-freedom aeroelastic model (with aerodynamic and structural damping) will be used in place of a generic host structure. All preceding derivations are applicable to this model, as will be discussed subsequently.

4. SHUNTED PIEZOELECTRICS APPLIED TO AN AEROELASTIC WING

4.1 Description of the analytical model

In this section, a simple two degree-of-freedom aeroelastic model is used to examine the feasibility of using shunted piezoelectrics to reduce aeroelastic response (see **Figure 5**). This type of model (analogous to the typical section models described in references 31 and) is useful in explaining the fundamental mechanisms of aeroelasticity. In the typical section model used herein, the shunted piezoelectrics were modeled as a damped vibration absorber, as shown in **Figure 5**. The aeroelastic equations of motion are first developed using the characteristics of the damped vibration absorber. Then, the terms representing the shunted piezoelectric are substituted in the equations of motion in place of the damped vibration absorber terms. In the model depicted in **Figure 5**, the mass, m_2 , stiffness, K_2 , and damping, C_2 , represent the damped vibration absorber, which is located at the elastic axis. The absorber is oriented to move in the “h” direction (wing bending or plunging of the elastic axis). Twist about the elastic axis is represented by the torsion (or pitching) degree-of-freedom, “ θ ”.

In this simplified idealization, the piezoelectrics are oriented to reduce the wing bending response due to the vertical motion of the damped vibration absorber. Vertical motion of the damped vibration absorber results in bending forces being applied to the wing section. Orienting the shunted piezoelectrics to affect bending response corresponds to orienting the “1” direction of the piezoelectric (see **Figure 1**) parallel to the elastic axis of the wing and, thus, perpendicular to the nodelines of the primary bending modes. A graphical depiction of this orientation is shown in **Figure 6**. This figure shows a very simplified depiction of a potential application of shunted piezoelectrics to reduce wing bending response. For actual application, the shunted piezoelectrics should be placed in the regions of highest strain for the modes of interest. More discussion of issues related to applying shunted piezoelectrics is provided subsequently. To affect torsion response on an orthotropic wing, the piezoelectrics shown in **Figure 6** would be rotated 90°. However, a more complex model than the one shown in **Figure 6** would be required to accurately examine the effects of shunted piezoelectrics oriented in such a manner since a “rotating” damped vibration absorber, or something similar, would have to be modeled. For the current study, only the effects of shunted piezoelectrics on bending response is considered.

4.2 Aeroelastic equations of motion with a damped vibration absorber

The dimensional aeroelastic equations of motion of the typical section model used with the damped vibration absorber were reduced, for simplicity, to include only the plunging and pitching aeroelastic equations of motion. This

simplification is accomplished by substituting the characteristics of the damped vibration absorber from the absorber equation of motion into the plunging and pitching aeroelastic equations of motion. Nondimensionalization of the equations of motion is attained by multiplying through by $1/(m_w \omega_h^2)$, where $\omega_h^2 = K_h/m_w$ is the uncoupled plunging natural frequency of the wing. It is important to note that, in most aeroelastic derivations, the equations of motion are nondimensionalized by multiplying through by $1/(m_{air} \omega^2)$. However, in the present study, nondimensionalization using $1/(m_w \omega_h^2)$ enables direct comparison between the aeroelastic equations of motion with shunted piezoelectrics and the equation of motion derived earlier for shunted piezoelectrics applied to a generic host structure. The

following nondimensional parameters were used in the nondimensional aeroelastic equations of motion: $r_\alpha^2 = \frac{I_\alpha}{m_w b^2}$;

$\omega_\alpha^2 = \frac{K_\theta}{I_\alpha}$; $\omega_2^2 = \frac{K_2}{m_2}$; $\Omega^2 = \frac{\omega_2^2}{\omega_h^2}$; $G^2 = \frac{\omega^2}{\omega_h^2}$; $\mu = \frac{m_w}{m_{air}}$; $M = \frac{m_2}{m_w}$; $C_c = 2m_2 \omega_h$; and, $\zeta = \frac{C_2}{C_c}$. The nondimensional

aeroelastic equations of motion can thus be written:

$$\left[\frac{-\left\{ M\Omega^2 G^2 - \left(G^2 \left(1 + \frac{L_h}{\mu} \right) - (1 + ig_h) \right) (G^2 - \Omega^2) \right\} - i2\zeta G \left(G^2 \left(1 + \frac{L_h}{\mu} \right) - (1 + ig_h) + MG^2 \right)}{-(G^2 - \Omega^2) + i2\zeta G} \right] \frac{\bar{h}}{b} - \left[G^2 \left(x_\alpha + \frac{L_\theta}{\mu} \right) \right] \bar{\theta} = 0 \quad (12)$$

$$\left[-G^2 \left(x_\alpha + \frac{M_h}{\mu} \right) \right] \frac{\bar{h}}{b} - \left[G^2 \left(r_\alpha^2 + \frac{M_\theta}{\mu} \right) - \frac{\omega_\alpha^2}{\omega_h^2} r_\alpha^2 (1 + ig_\theta) \right] \bar{\theta} = 0$$

Structural damping, g , is approximated assuming small damping forces that are opposite in phase to velocity and directly proportional to the elastic restoring force. In addition, simple harmonic motion is assumed thus, the degrees of freedom and aerodynamic lift and pitching moment can be written:

$h = \bar{h}e^{i\omega t}$, $\theta = \bar{\theta}e^{i\omega t}$, $x_2 = \bar{x}_2 e^{i\omega t}$, $L_A = \bar{L}_A e^{i\omega t}$, $M_A = \bar{M}_A e^{i\omega t}$ where the barred terms (i.e., \bar{h}) represent the amplitude and phase angle of each term.

The aerodynamic lift and pitching moment were developed using Theodorsen's exact aerodynamic solution.³¹⁻³³ Thus, the aerodynamic lift and pitching moment are defined:

$$\bar{L}_A = -\pi\rho b^3 \omega^2 L_h \frac{\bar{h}}{b} - \pi\rho b^3 \omega^2 \left(L_\alpha - \left(\frac{1}{2} + a \right) L_h \right) \bar{\theta} \quad (13)$$

$$\bar{M}_A = -\pi\rho b^4 \omega^2 \left(M_h - \left(\frac{1}{2} + a \right) L_h \right) \frac{\bar{h}}{b} - \pi\rho b^4 \omega^2 \left(M_\alpha - \left(\frac{1}{2} + a \right) (L_\alpha + M_h) + \left(\frac{1}{2} + a \right)^2 L_h \right) \bar{\theta}$$

In the above equations, L_h , L_α , M_h , and M_α , are functions of Theodorsen's function, $C(k)$, where k is the reduced frequency defined as: $k = \omega b/V$. Note that Theodorsen's representation of the aerodynamic forces includes aerodynamic damping. To simplify the aerodynamic lift and pitching moment equations, the following substitutions are used: $m_{air} = \pi\rho b^2$; $L_\theta = L_\alpha - \left(\frac{1}{2} + a \right) L_h$; $M_h = M_h - \left(\frac{1}{2} + a \right) L_h$; and, $M_\theta = M_\alpha - \left(\frac{1}{2} + a \right) (L_\alpha + M_h) + \left(\frac{1}{2} + a \right)^2 L_h$.

Equation 12 represent the pitch and plunge equations of motion of a typical wing section with a damped vibration absorber placed on the elastic axis (shown in **Figure 5**). Notice that in examining equation 13, it is apparent that the only differences between the aeroelastic equations of motion derived above and the equation describing the lumped parameter system in Figure 3 (equation 6) are the addition of the aerodynamic forces and the torsional characteristics of the wing. As discussed earlier, the damped vibration absorber can be used to represent shunted piezoelectrics with two important modifications to the nondimensional equations of motion. These are: 1) substituting the squared generalized electro-mechanical coupling coefficient, \bar{K}_{31}^2 , for the $M\Omega^2$ terms; and 2) removing the terms containing $i2\zeta MG^3$.

4.3 Aeroelastic equations of motion with shunted piezoelectrics

Making the aforementioned modifications to the aeroelastic equations of motion yields:

$$\left[\frac{-\left\{ \bar{K}_{31}^2 G^2 - \left(G^2 \left(1 + \frac{L_h}{\mu} \right) - (1 + ig_h) \right) (G^2 - \Omega^2) \right\} - i2\zeta G \left(G^2 \left(1 + \frac{L_h}{\mu} \right) - (1 + ig_h) \right)}{-(G^2 - \Omega^2) + i2\zeta G} \right] \frac{\bar{h}}{b} - G^2 \left(x_\alpha + \frac{L_\theta}{\mu} \right) \bar{\theta} = 0 \quad (14)$$

$$\left[-G^2 \left(x_\alpha + \frac{M_b}{\mu} \right) \right] \frac{\bar{h}}{b} - \left[G^2 \left(r_\alpha^2 + \frac{M_\theta}{\mu} \right) - \frac{\omega_\alpha^2}{\omega_h^2} r_\alpha^2 (1 + ig_\theta) \right] \bar{\theta} = 0$$

These equations can also be simply written as:

$$\begin{bmatrix} \bar{A} & \bar{B} \\ \bar{D} & \bar{E} \end{bmatrix} \begin{Bmatrix} \frac{\bar{h}}{b} \\ \bar{\theta} \end{Bmatrix} = \begin{Bmatrix} 0 \\ 0 \end{Bmatrix} \quad (15)$$

Note that the electrical properties of the shunted piezoelectric are represented by using the nondimensional terms defined previously for a generic host structure with shunted piezoelectrics (see equation 5) : $\zeta = 1/(2RC^S\omega_h)$, $\Omega^2 = \omega_E^2/\omega_h^2$, $\bar{K}_{31}^2 = (\omega_{OC}^2 - \omega_h^2)/\omega_h^2$. In these equations the identity, $\omega_{SC} = \omega_h$, has been introduced since the short circuit natural frequency, ω_{SC} , is the natural frequency of the wing including piezoelectrics without any external electrical stimulus such as a shunt circuit. In addition, it follows that the inductance and resistance are defined:

$$L = 1/(\omega_h^2 \Omega^2 C^S) \quad R = 1/(2\omega_h C^S |\zeta|) \quad (16)$$

Using equation 14, the effectiveness of the shunted piezoelectrics to reduce aeroelastic response can be examined. Optimal reduction in aeroelastic response can be obtained by using the tuning methodologies discussed previously. In the next section, computer simulations of the typical model used herein is employed to examine the effectiveness of the shunted piezoelectrics to reduce aeroelastic response at subcritical speeds (speeds below flutter). Examination of the impact of shunted piezoelectrics on flutter values was beyond the scope of the current work.

5. COMPUTER SIMULATIONS

5.1 Flutter analysis to establish the stability boundary

To examine the effectiveness of the shunted piezoelectrics, analytical simulations of the typical section model described above were developed using MATLAB.³⁴ The following parameters were used for all of the subsequent analyses: $\mu = 40$, $r_\alpha^2 = 0.6$, $x_\alpha = 0.15$, $a = -0.25$, $b = 3$ ft. Two aeroelastic models were examined. For each model, the aeroelastic response with and without structural damping (g_h and g_θ) was considered. Initially, a flutter analysis of each aeroelastic model without the shunted piezoelectrics was conducted to establish the stability boundary and to select the subcritical speeds for the response reduction simulations. Removing the effect of the shunted piezoelectrics in the flutter analysis was accomplished by setting: $M=\Omega=\zeta=0$. Two different flutter analysis methods were used to verify the final flutter values for each model; both methods yielded approximately the same flutter values for each model. The k method (also called American method) and the P-k (or British method) were employed. Table 1 summarizes the parameters used for the models and their calculated flutter speeds and frequencies.

Table 1 Parameters for aeroelastic models used in computer simulations and flutter values

Model name	ω_h	ω_θ	gh	g θ	Flutter speed (ft/sec)	Flutter frequency (rad/sec)
1a	12	40	0.0	0.0	517	28.3
1b	12	40	0.03	0.03	537	26.9
2a	20	40	0.0	0.0	446	31.3
2b	20	40	0.03	0.03	464	30.1

5.2 Forced response analysis

The effectiveness of the shunted piezoelectrics to reduce response was examined at five subcritical velocities. The velocities used for models 1a and 1b were 100, 200, 280, 330, and 380 ft/sec. The velocities used for models 2a and 2b were 70, 150, 220, 285, and 330 ft/sec. The velocities were chosen by considering that, for a typical airplane, the maximum dive speed is usually 20% less than the flutter speed and the maximum cruise speed is typically 20% less than the maximum dive speed. For example, maximum cruise speed for model 1a would be approximately 330 ft/sec. In choosing the other velocities, three values of velocity below the maximum cruise speed were considered to encompass the wide range of speeds a typical airplane might experience in its flight envelope. One velocity above the maximum cruise speed was also considered to explore response reduction at speeds outside the typical flight envelope.

Effectiveness of the shunted piezoelectrics at the aforementioned speeds was examined by studying the response of the typical section models to sinusoidal forcing functions, P (plunge force) and T (torsion moment). Assuming simple harmonic motion, P and T can be written: $P = \bar{P}_o e^{i\omega t}$ and $T = \bar{T}_o e^{i\omega t}$. These forcing functions were first nondimensionalized using the same quantities used in equation 13 to obtain: $\bar{p}_o = \bar{P}_o / (m_w \omega_h^2)$ and $\bar{t}_o = \bar{T}_o / (m_w \omega_h^2)$. To further simplify the simulation results, the plunging and pitching responses were normalized by static deflections.

The static plunging and pitching deflections are given by: $\bar{h}_{st} = \frac{\bar{p}_o}{b}$ and $\bar{\theta}_{st} = \frac{\bar{t}_o}{b^2} \frac{\omega_h^2}{\omega_\alpha^2 r_\alpha^2}$. The resulting normalized responses are:

$$\frac{\bar{h}}{\bar{h}_{st}} = \frac{\bar{E} - \frac{\bar{t}_o}{\bar{p}_o} \bar{B}}{\Delta} \quad \frac{\bar{\theta}}{\bar{\theta}_{st}} = \frac{\omega_\alpha^2 r_\alpha^2}{\omega_h^2} \left(\frac{\bar{A} - \frac{\bar{p}_o b}{\bar{t}_o} \bar{D}}{\Delta} \right) \quad (17)$$

where Δ is the determinant of the matrix $\begin{bmatrix} \bar{A} & \bar{B} \\ \bar{D} & \bar{E} \end{bmatrix}$ from equation 15.

In addition, the following values for plunging and pitching deflections were used for all of the models examined: $\bar{h}_{st} = 0.75$ feet, $\therefore \bar{p}_o = 0.75$ and $\bar{\theta}_{st} = 2^\circ$ $\therefore \bar{t}_o = 2.09$. The normalized wing responses given in equation 17 will be used throughout the remaining analyses. The subcritical response of the aeroelastic models, with and without the shunted piezoelectrics, will be examined considering a linear sweep of the frequency of the forcing functions from 9 rad/sec to 45 rad/sec. Furthermore, as discussed previously, since the shunted piezoelectrics considered herein were oriented to reduce plunging (bending) response, the model used is not sufficient for a reliable, quantitative analysis of pitching (torsion) response reduction. Thus, only the normalized plunge response will be emphasized in the computer simulations.

5.3 Tuning the shunt circuit to reduce aeroelastic response

With the typical section properties and forcing function parameters fixed, the only remaining parameters are those relating to the shunted piezoelectrics, namely \bar{K}_{31} , Ω , and ζ . As mentioned previously, the generalized electro-

mechanical coupling coefficient, \bar{K}_{31} , is primarily a function of how well the piezoelectrics are bonded to the host structure. Assuming that all piezoelectrics used in the current study were bonded using currently available bonding materials and techniques, one (typical) value of \bar{K}_{31} was used for all of the analyses: $\bar{K}_{31} = 0.12$.

As shown earlier, the frequency ratio, Ω , and the damping ratio, ζ , are the two critical parameters that determine the effectiveness of the shunted piezoelectrics. These quantities determine the value of capacitance (the piezoelectrics), resistance, and inductance in the shunt circuit and can be tuned to optimize the vibration reduction of the host structure. However, the wing used herein includes both aerodynamic damping and structural damping. The methodology shown earlier for tuning the shunt circuit can be applied to systems with damping by either: 1) neglecting the damping that exists in the host structure and solving for the optimal frequency and damping ratio; or 2) using an iterative computational procedure where the damping in the host structure is included as the tuning parameters are found. As mentioned previously, both methods should yield similar results. The former method is not desirable for the aeroelastic system since excluding the aerodynamic damping to seek closed-form solutions for optimum frequency and damping ratio would lead to inaccuracies in the calculation of the aeroelastic response. Thus, the latter approach of using a simple, computer-based iterative procedure was implemented. Table 2 summarizes the optimal values found for each model using a computational, iterative procedure.

Table 2 Optimal frequency and damping ratios

Model name	Velocity (ft/sec)	Ω_{opt}	ζ_{opt}
1a	100	.9906	.0776
	200	1.0046	.0848
	280	1.0170	.0932
	330	1.0233	.0974
	380	3.0122	.0251
1b	100	.9894	.0793
	200	1.0032	.0868
	280	1.0158	.0938
	330	1.0234	.0986
	380		
2a	70	.9801	.0730
	150	.9895	.0766
	200	.9987	.0793
	285	1.0224	.0853
	330	1.0406	.0898
2b	70	.9792	.0750
	150	.9884	.0783
	200	.9977	.0809
	285	1.0219	.0868
	330	1.0414	.0914

In examining Table 2, note that except at 380 ft/sec for models 1a and 1b, the variation in optimum frequency ratio with airspeed is not significant. This is due to the small variation in the plunge natural frequency with airspeed, which is an indicator that a passive shunt circuit might be effective in reducing plunge response. In addition, an approximate verification of the values in Table 2 can be made by comparing with the values obtained using the empirical solutions for optimal frequency and damping ratio derived earlier for a generic structure. Recall that the only difference between the previous development using a generic structure and the current development using a

wing is the addition of a coupled, torsional degree-of-freedom and aerodynamics on the wing. Using equations 7 and 9, the optimal frequency ratio and the magnitude of the optimal damping ratio are 0.996 and 0.0725, respectively. These values are very close to the values in Table 2 except at 380 ft/sec for models 1a and 1b. The optimal damping ratio at this airspeed is very low, which may indicate that the damped vibration absorber analogy is no longer valid at this airspeed for this wing. More discussion on the significance of the above optimal tuning results will be given after an examination of the response reduction results in the next section.

5.4 Results of forced response analysis

The responses of the wing models were calculated with and without shunted piezoelectrics at each airspeed. Sample plots of the bending response at 200 ft/sec for model 1a is shown in Figure 7 and for model 2a in Figure 8. As expected, these plots closely resemble the plots shown in Figure 4 of the shunted piezoelectrics applied to a generic host structure. In both cases, the shunted piezoelectric creates a “double hump” in the magnitude of the response and, consequently, two 90° drop-offs in the phase. Also, note that in Figures 7 and 8 the response is plotted using the optimal tuning values as well as the non-optimal tuning values for another airspeed. Although use of the optimal tuning values clearly yields the best response reduction, use of the non-optimal tuning values yields considerable response reduction as well. Using plots such as these for each airspeed, the percent reduction in the peak plunging response using the shunted piezoelectrics can be calculated. Overall, the shunted piezoelectrics were very effective in reducing the plunge response of the typical section models considered; a 10% to 70% reduction was calculated for the range of airspeeds considered, except at 380 ft/sec for models 1a and 1b.

In general, the effectiveness of the shunted piezoelectrics is largely a function of the percent of inherent aeroelastic damping the shunted system can add using the optimum frequency and damping ratios. That is, the more damping that already exists in the aeroelastic system, the less effective the shunted piezoelectric. This characteristic is displayed in the results in several ways:

- 1) The overall decrease in the effectiveness of the shunted piezoelectrics with airspeed for all of the models.
- 2) The overall decrease in effectiveness with added inherent structural damping, g_θ and g_h . This is evident by comparing the responses of model 1a with model 1b, and comparing responses of model 2a with model 2b.
- 3) The general increase in effectiveness for models 2a and 2b as compared to models 1a and 1b.

In examining the first item above, note that a common characteristic of aeroelastic systems is small damping at low airspeeds and increased damping with airspeed. For the mode that goes unstable, this characteristic is followed by a reverse in the damping trend near the flutter speed, toward zero damping at flutter.³¹ Thus, the overall decrease in the effectiveness of the shunted piezoelectric with increased airspeed is due to the increased inherent aerodynamic damping with airspeed. Figure 9 shows this trend clearly. In this figure, the results for the models with and without structural damping are plotted for actively shunted piezoelectrics. Thus, the only damping present for the models without structural damping (models 1a and 2a) is due to the aerodynamics and the shunted piezoelectric.

The second item in the list above addresses the impact of adding inherent structural damping, g_θ and g_h . In comparing the responses in Figure 9, note that the only difference of the “b” models over the “a” models is the addition of inherent structural damping, g_θ and g_h (see Table 1). This additional damping reduces the response for the “b” models at all airspeeds, and thus results in the shunted piezoelectrics being less effective for the “b” models. Although the reduction in effectiveness was not considerable for the models considered, the impact of inherent structural damping cannot be ignored since this quantity can vary significantly for aeroelastic structures.

The last item in the list above addresses the comparison between models 1a and 1b with models 2a and 2b. Overall, the plunge responses of models 2a and 2b were less damped than models 1a and 1b, resulting in the shunted piezoelectrics being more effective on models 2a and 2b. This is not surprising considering that models 2a and 2b are generally less stable than models 1a and 1b, as is evident by examining their flutter characteristics and comparing the responses shown in Figures 9 and 10.

Another important issue in examining the results is the impact of using non-optimum frequency and damping ratios. As mentioned previously, passive use of the shunt circuit would imply tuning the circuit for one condition and using these tuning values for the entire flight envelope. To simulate this in the current study, it was assumed that the shunt circuit would be tuned for the maximum cruise condition and these optimum (tuning) values would be used at the other speeds. The passive shunt circuit was less effective than the active shunt circuit at every airspeed except the maximum cruise speed. This characteristic is shown in Figure 10 where the response with an active shunt circuit is compared with that of a passive shunt circuit. The effectiveness of the passive shunt circuit depends primarily upon the variation of plunge natural frequency. Thus, at velocities far from the maximum cruise condition, the impact of using off-tuned values was most significant (as much as a 20% drop in effectiveness). On the other hand, considering the simplicity of a passive shunt circuit and that this circuit is still 80% as effective as the active circuit at worst conditions, the passive shunt circuit may be a desirable approach for some aeroelastic applications.

The reduction of the pitch response due to the shunted piezoelectrics was essentially negligible, as anticipated; approximately 0.2% reduction for models 1a and 1b and 1.5% reduction for models 2a and 2b. As with the reductions in plunge responses, the reductions in pitch response increased slightly as the natural frequency of the shunt circuit got closer to the natural pitch frequency.

Lastly, $V=380$ ft/sec for models 1a and 1b represents a unique case. At this condition only, the plunge due to pitch response (the flutter mode) dominates the overall plunge response. At this speed, the shunt circuit was tuned for the plunge due to pitch mode as opposed to the plunge natural mode (see Table 2). However, recall that the shunted piezoelectrics were oriented to reduce plunge response only. Thus, examination of the effectiveness of the shunted piezoelectrics on the plunge due to pitch response is probably beyond the realistic usability of the simple lumped parameter idealization used. Correspondingly, the response at this speed was significantly different from the responses at the other speeds where the shunt circuit was tuned for the plunge natural mode. For example, the response was uncharacteristically very sensitive to variations in frequency and damping ratios; thus, tuning at this speed was quite difficult. Recall that the responses of models 1a and 1b were calculated using the same optimal frequency and damping ratio because, structural damping typically does not significantly affect these values. However, the addition of structural damping resulted in the shunted piezoelectrics being significantly off-tuned for model 1b. Moreover, in reviewing Table 2, note that the damping ratio for $V=380$ ft/sec is very low. As mentioned previously, simulation of the shunted piezoelectric at very low damping ratios using a damped vibration absorber analogy may be inaccurate. Thus, further investigation of the behavior of the typical section with shunted piezoelectrics for coupled modes with low damping ratio is required before reliable conclusions can be reached for these conditions.

Overall, the shunted piezoelectrics were very effective in reducing plunge response using both a passive and active shunt circuit. At the unique condition of $V=380$ ft/sec for models 1a and 1b, the effect of the shunted piezoelectrics is uncertain and requires further investigation. At all other speeds, the shunted piezoelectrics reduced the response of all modes, although the impact on pitch modes was not significant due to the orientation of the shunted piezoelectrics for the current study.

6. APPLICATION ISSUES AND RECOMMENDATIONS FOR FUTURE WORK

The preceding analysis examined the application of shunted piezoelectrics to a simple two-degree-of-freedom model of an aeroelastic system. While this analysis clearly shows that shunted piezoelectrics can reduce aeroelastic response, considerable additional research is required before shunted piezoelectrics can be applied to realistic air vehicles for aeroelastic response reduction. This research includes developing improved analytical models and experimental validation. Limited (unpublished) data on the use of shunted piezoelectrics on air vehicles is available. Wind-tunnel tests are tentatively planned to further assess using shunted piezoelectrics for aeroelastic response reduction. In an actual application, shunted piezoelectrics will likely be most effective if they are designed into the

structure, as opposed to being used as a retrofit. To effectively design shunted piezoelectrics into a structure the following considerations must be addressed: maximize the strain energy transfer from the host structure to the piezoelectric and maintain structural integrity. These objectives can often have conflicting requirements. To achieve the first objective, for example, the piezoelectrics are placed in the high-strain regions of the host structure as indicated by examination of the mode shapes of interest. However, piezoelectric materials, as compared to traditional load-carrying materials, have an lesser load-carrying capability.²⁴ Thus, piezoelectric materials should not be relied upon as critical load-carrying structural components and thus must be carefully designed into the host structure. These design considerations are also applicable to applications where piezoelectrics are used as actuators.

Sensing equipment is also necessary to use shunted piezoelectrics. The frequency of the mode of interest on the host structure and the natural frequency of the shunt circuit must be accurately measured to tune the shunt circuit. For active shunting, sensing must be continuous. For passive shunting, sensing equipment is only needed in the initial tuning of the shunt circuit.

Another important issue that must be addressed for realistic aeroelastic application is ensuring the robustness the shunted piezoelectrics as the natural frequency of the air vehicle varies. To address the issue of varying natural frequencies on the host structure, some researchers have examined “self-tuning” shunt circuits to retune the circuits as the natural frequency of the host structure varies.^{14, 15} These self-tuning circuits (or active shunting) behave like an active control system: given an input (the short circuit natural frequency, ω_{SC}), an active control law determines the optimal frequency and damping ratios needed to optimally reduce the response. Alternatively, if modal response in a specific portion of the flight envelope is of most importance, the shunt circuit can be tuned a priori for the flight condition of interest and shunted piezoelectrics can be used passively. In this application, the shunted piezoelectrics still dissipate energy at conditions other than the one of interest; however, the shunted piezoelectrics are most effective at the flight condition for which they were tuned. Another method to consider is designing the shunted piezoelectric to reduce response in more than one mode simultaneously. This method, examined in references 13, 16, and 20, may prove to be very useful for air vehicles that have multiple modes contributing to an unacceptably large response. The above approaches have the added advantage of accomodating the variation of piezoelectric capacitance with voltage.

Finally, in general, increasing the damping in a structure has the primary effect of reducing vibration amplitudes at resonances. This can lead to reduced displacements, stresses, fatigue and noise. In addition, references 9 and 35 observe that damping can also add robustness and stability to marginally-stable active control systems which, in turn, can reduce the chance of spillover that can destabilize a system. Thus, shunting a piezoelectric and actuating it using a control law may provide a highly robust and very effective vibration control approach.

7. CONCLUSIONS

The feasibility of using shunted piezoelectrics to reduce aeroelastic response at speeds below flutter was examined via analysis. The piezoelectrics used in this study were shunted using a parallel resistor and inductor. Examination of this shunt circuit applied to a generic host structure was first studied to assess the general characteristics of this application and the limitations of the current analytical methods. These developments were used as a basis for applying shunted piezoelectrics to a typical-section aeroelastic model. Using Theodorsen aerodynamics, the response of two aeroelastic models to sinusoidal forcing functions was examined to study the effectiveness of using shunted piezoelectrics to reduce aeroelastic response. These results demonstrate that shunted piezoelectrics can significantly reduce aeroelastic response; for example, reductions of up to 70% in plunging response were realized. The effectiveness of the shunted piezoelectrics was found to be a strong function of the inherent structural and aerodynamic damping. Thus, this application may not be effective for highly damped structures. However, for lightly damped structures, shunted piezoelectrics provide a simple, low-power, fail-safe vibration suppression mechanism. Follow-on studies are planned to explore developing higher fidelity models and to validate the results via wind-tunnel testing.

ACKNOWLEDGEMENTS

The author would like to acknowledge the invaluable discussions with Drs. Chuh Mei, Donald Kunz, Ray Kvaternik, Robert Bennett, Jim Wu, and Ms. Jennifer Heeg.

REFERENCES

- ¹ Weisshaar, T.A., "Aeroservoelastic Control with Active Materials- Progress and Promise," CEAS International Forum on Aeroelasticity and Structural Dynamics, Manchester UK, June 1995.
- ² Crowe, C. R. and Sater, J. M., "Smart Aircraft Structures," Future Aerospace Technology in the Service of the Alliance, Vol. 1: Affordable Combat Aircraft, AGARD Conference Proceedings 600, pp. A20-1 to A20-15, Paris, France, 1997.
- ³ Loewy, R.G., "Recent Developments in Smart Structures with Aeronautical Applications," Journal of Smart Materials and Structures, Vol. 5, October 1997, pp. 11-41.
- ⁴ Hopkins, M.A., Henderson, D.A., Moses, R.W., Findlay, D., Voracek, D.F., Spangler, R.L., Ryall, T., and Zimcik, D., "Active Vibration Suppression Systems Applied to Twin Tail Buffeting," Proceedings of SPIE's 5th Annual Symposium on Smart Structures and Materials, Paper No. 3326-05, San Diego, CA, March 1-5, 1998.
- ⁵ Moses, R.W., "Active Vertical Tail Buffeting Alleviation on a Twin-Tail Fighter Configuration in a Wind Tunnel," Proceedings of the CEAS International Forum on Aeroelasticity and Structural Dynamics 1997, Rome, Italy, 1997.
- ⁵ Pinkerton, Jennifer L. and Moses, Robert W., "A Feasibility Study To Control Airfoil Shape Using THUNDER", NASA TM-4767, November 1997.
- ⁶ McGowan, A. R., Heeg, J., and Lake, R.C., "Results of Wind-Tunnel Testing From the Piezoelectric Aeroelastic Response Tailoring Investigation," Proceedings of the 37th AIAA/ASME/ASCE/AHS/ASC Structures, Structural Dynamics and Materials Conference, Salt Lake City, UT, April 1996.
- ⁷ Brennan, M. C. and McGowan, A. R., "Piezoelectric Power Requirements for Active Control," Proceedings of the SPIE's 4th Annual Symposium on Smart Structures and Materials, Mathematics and Control in Smart Structures Conference, Paper 3039-69, March 1997.
- ⁸ McGowan, A. R., "A Feasibility Study of Using Shunted Piezoelectric Piezoelectrics to Reduce Aeroelastic," SPIE's 6th Annual Symposium on Smart Structures and Materials, Industrial and Commercial Applications Conference, Newport Beach, CA Paper number 3674-20, March 1999.
- ⁹ Agnes, G.S., "Active/Passive Piezoelectric Vibration Suppression," Proceedings of the 1994 SPIE Smart Structures and Materials, Passive Damping Conference, Orlando, FL, Vol. 2193, Feb. 14-16, 1994, pp. 24-34.
- ¹⁰ Hagood, N.W., IV, and von Flotow, A.H., "Damping of Structural Vibrations with Piezoelectric Materials and Passive Electrical Networks," Journal of Sound and Vibration, Vol. 146, No. 2, 1991, pp. 243-268.
- ¹¹ Forward, R. L., "Electronic Damping of Vibrations in Optical Structures," Journal of Applied Optics, Vol. 18, No. 5, March 1979, pp. 690-697.
- ¹² Edberg, D.L., Bicos, A.S., and Fetcher, J.S., "On Piezoelectric Energy Conversion for Electronic Passive Damping Enhancement," Proceedings of Damping '91, San Diego, CA, Paper GBA-1, Feb. 1991.
- ¹³ Hollkamp, J.J., "Multimodal Passive Vibration Suppression with Piezoelectrics," Proceedings of the 34th AIAA/ASME/ASCE/AHS /ASC Structures, Structural Dynamics, and Materials Conference and AIAA/ASME Adaptive Structures Forum, La Jolla, CA, Apr. 19-22, 1993, Paper number: AIAA 93-1683-CP, pp. 3227-3237.
- ¹⁴ Hollkamp, J.J., and Starchville, T.F., "A Self-Tuning Piezoelectric Vibration Absorber," Proceedings of the AIAA/ASME Adaptive Structures Forum, Hilton Head, SC, Apr. 21-22, 1994, pp. 521-529.
- ¹⁵ Wang, K.W., Yu, W.K., and Lai, J.S., "Parametric Control of Structural Vibrations via Piezoelectric Materials Shunted with Adaptive Circuits," Proceedings of the Conference on Smart Structures and Materials 1994: Mathematics and Control in Smart Structures," Orlando, FL, Vol. 2192, Feb. 14-16, 1994, pp. 120-131.
- ¹⁶ Agnes, G. S., "Development of a modal model for simultaneous active and passive piezoelectric vibration suppression." Journal of Intelligent Material Systems and Structures, Vol. 6(4), 1995, pp. 482-487.

- 17 Yarlagadda, S., Lesieutre, G.A., Yoshikawa, S., and Witham, J., "Resistively Shunted Piezocomposites for Passive Vibration Damping," AIAA Paper No. A96-27071 06-39, Proceedings of the AIAA/ASME/AHS Adaptive Structures Forum, Salt Lake City, UT, Apr. 18-19, 1996, pp. 217-227.
- 18 Wu, S., "Piezoelectric Shunts with a Parallel R-L Circuit for Structural Damping and Vibration Control," Proceedings of SPIE's Symposium on Smart Materials and Structures, Vol 2720, March 1996, pp. 259-269.
- 19 Wu, S., and Bicos, A.S., "Structural Vibration Damping Experiments Using Improved Piezoelectric Shunts," Proceedings of the SPIE's 5th Annual Symposium on Smart Structures and Materials, Passive Damping and Isolation Conference, San Diego, CA, Vol. 3405, Mar. 3-4, 1997, pp. 40-50.
- 20 Wu, S.Y., "Method for Multiple Mode Shunt Damping of Structural Vibration Using a Single PZT Transducer," Proceedings of SPIE's 6th Annual Symposium on Smart Structures and Materials, Vol. 3327, March 1998.
- 21 Smith, C.A., and Anderson, E.H., "Passive Damping by Smart Materials: Analysis and Practical Limitations," Proceedings of the Smart Structures and Materials Symposium, Passive Damping and Isolation Conference, Vol. 2445, San Diego, CA, Mar 1-2, 1995, pp. 136-148.
- 22 Hollkamp, J.J., and Gordon, R.W., "An Experimental Comparison of Piezoelectric and Constrained Layer Damping," Proceedings of the Smart Structures and Materials Symposium, Passive Damping and Isolation Conference, Paper No. A95-37751 10-39, San Diego, CA, Vol. 2445, Mar. 1-2, 1995, pp.123-133.
- 23 Hagood, N.W., IV, Aldrich, J.B., and von Flotow, A.H., "Design of Passive Piezoelectric Damping for Space Structures," Final Report, NASA CR 4625, September 1994.
- 24 Agnes, G.S., and Inman, D.J., "Nonlinear Piezoelectric Vibration Absorbers," Journal of Smart Materials and Structures, Vol. 5, Issue 5, Oct. 1996, pp. 704-714.
- 25 IEEE Standard on Piezoelectricity, Standard 176-1987, 1987, New York, NY.
- 26 Crawley, E.F., and DeLuis, J., "Use of Piezoelectric Actuators as Elements of Intelligent Structures," AIAA Journal, Vol. 25, No. 10, 1987, pp. 1373-1385.
- 27 Den Hartog, J.P., Mechanical Vibrations, Fourth Edition, McGraw-Hill Book Company, Inc, New York, New York, 1956.
- 28 Ormondroyd, J., and Den Hartog, J.P., "The Theory of the Dynamic Vibration Absorber," May 1928, Transactions of the ASME, APM-50--7, pp. 9-22.
- 29 Timoshenko, S., and Young, D.H., Vibrations Problems in Engineering, Third Edition, D. Van Nostrand Company, Inc., Princeton, New Jersey, 1955.
- 30 Hunt, J. B., Dynamic Vibration Absorbers, Mechanical Engineering Publications, Ltd., London, England, 1979.
- 31 Bisplinghoff, R.L., Ashley, H., and Halfman, R.L., Aeroelasticity, Addison-Wesley Publishing Company, Inc., Reading, Massachusetts, 1955.
- 32 Fung, Y.C., An Introduction to the Theory of Aeroelasticity, Dover Publications, Inc., New York, 1969.
- 33 Theodorsen, T., "General Theory of Aerodynamic Instability and the Mechanism of Flutter," NACA Rrt 496, 1935.
- 34 Using MATLAB, The Mathworks, Inc., 1997.
- 35 Ashley, H. Edberg, D., "On the Virtues and Prospects for Passive Damping in Large Space Structures," Proceeding of Damping '86, AFWAL-TR-86-3059, Vol. 1, May 1986.

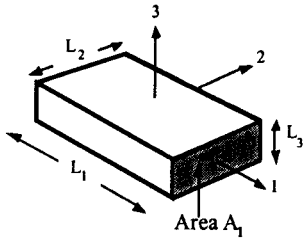


Figure 1. Typical piezoelectric element

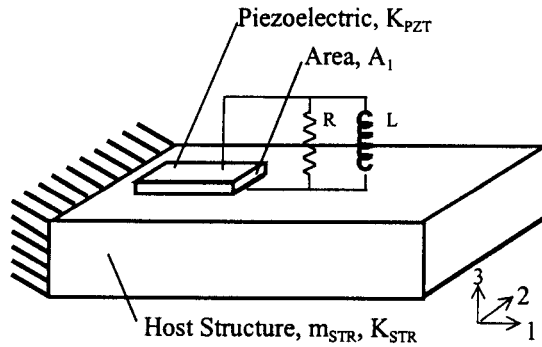


Figure 2. Generic host structure with a shunted piezoelectric

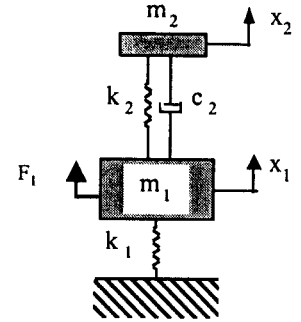


Figure 3. A damped vibration absorber attached to a host structure

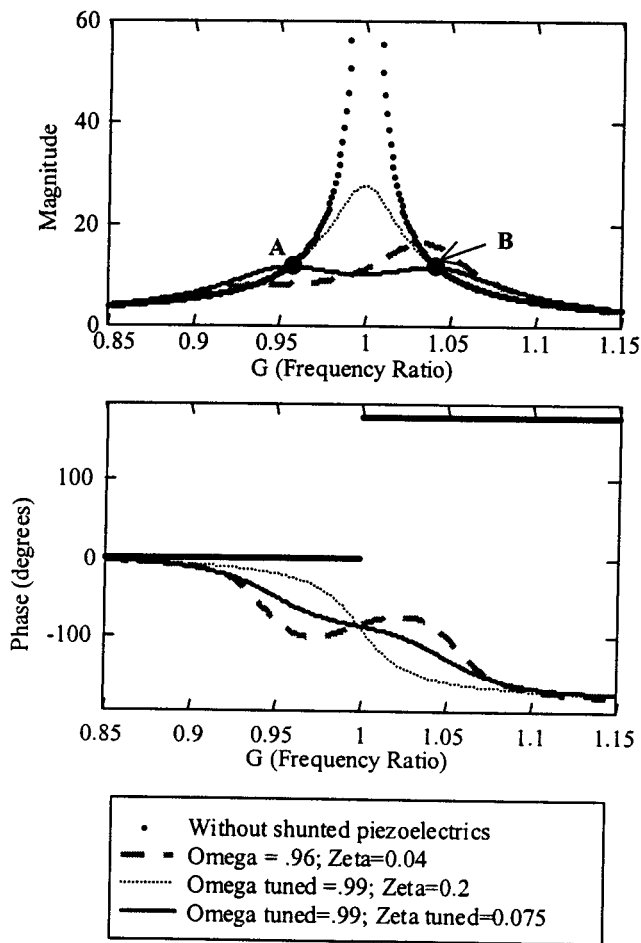


Figure 4. Response of host structure with attached shunted piezoelectrics

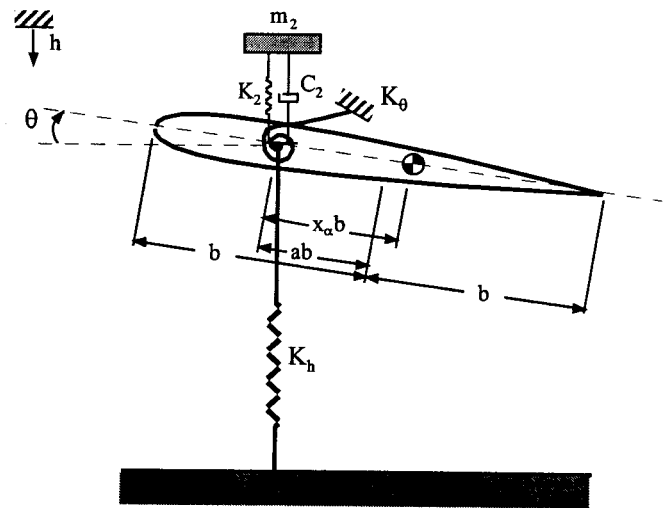


Figure 5. Typical section model

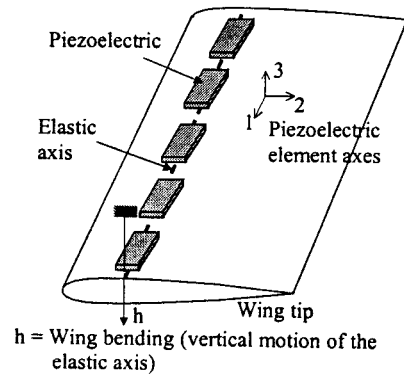


Figure 6. Example applications of shunted piezoelectrics on a wing

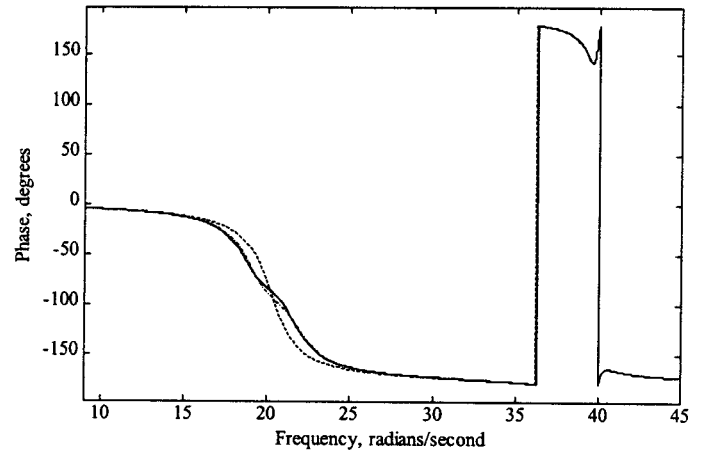
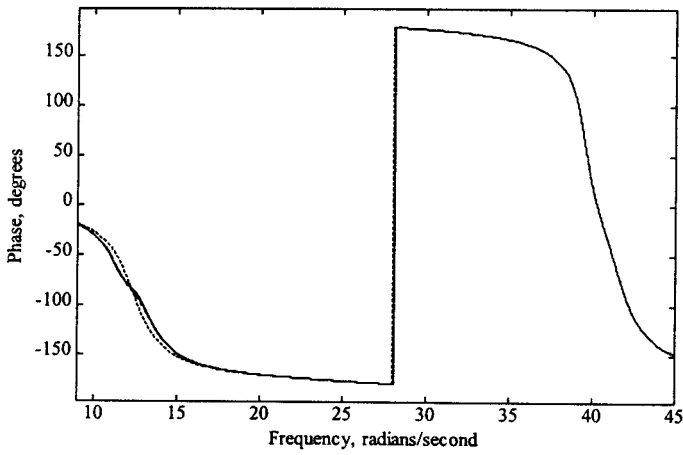
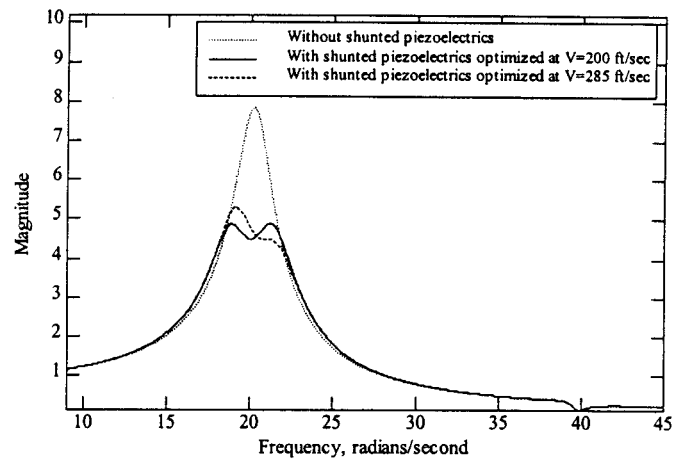
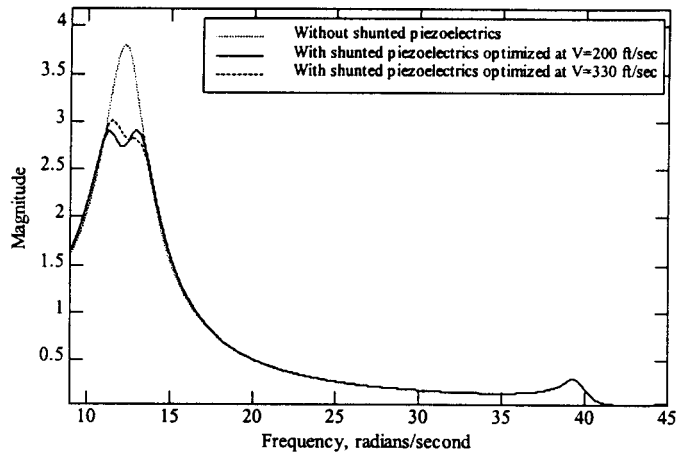


Figure 7. Nondimensional plunge response for model 1a at 200 ft/sec

Figure 8. Nondimensional plunge response for model 2a at 200 ft/sec

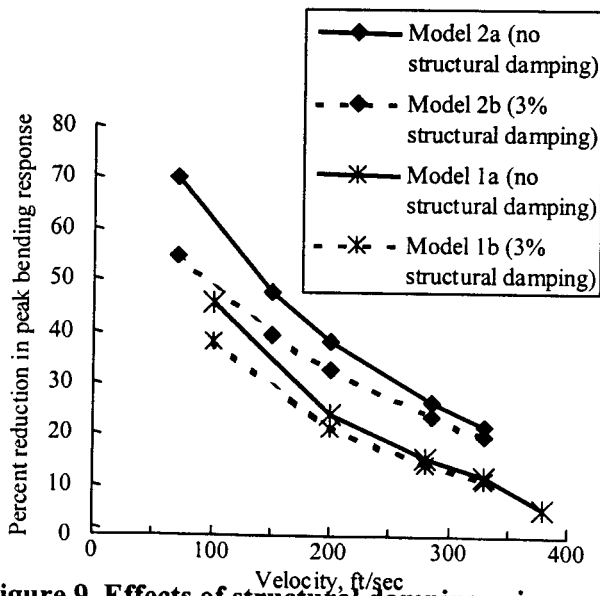


Figure 9. Effects of structural damping using models that are actively shunted

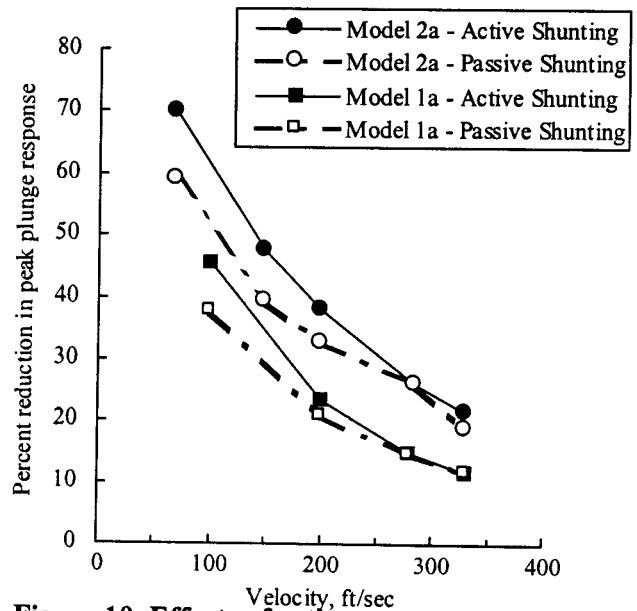


Figure 10. Effects of active versus passive shunting using models with no structural damping

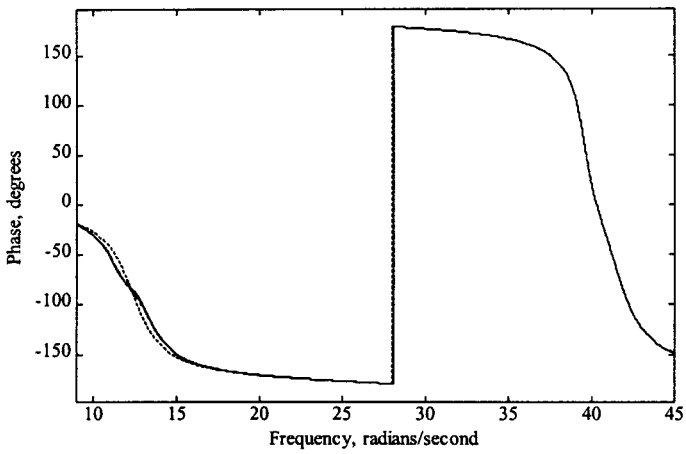
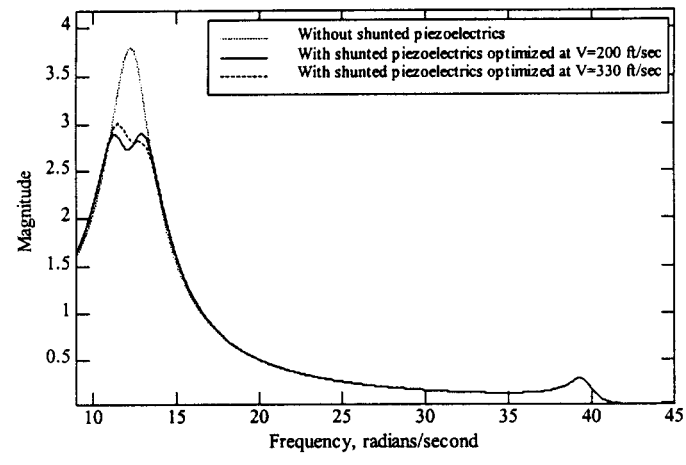


Figure 7. Nondimensional plunge response for model 1a at 200 ft/sec

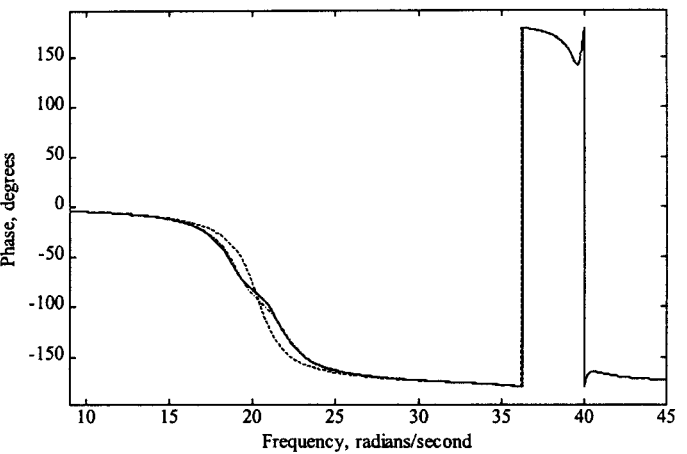
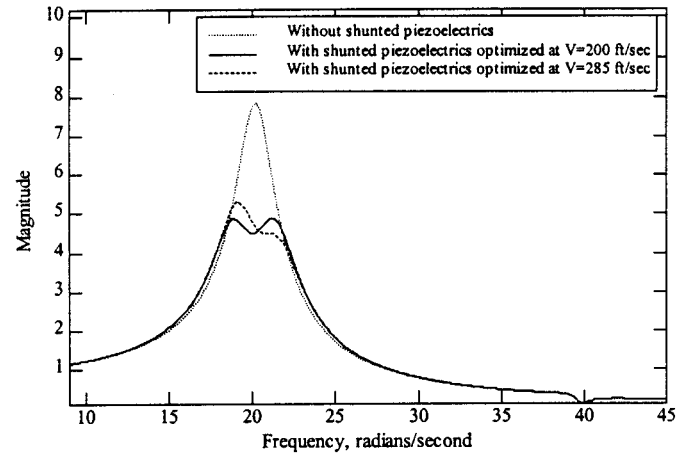


Figure 8. Nondimensional plunge response for model 2a at 200 ft/sec

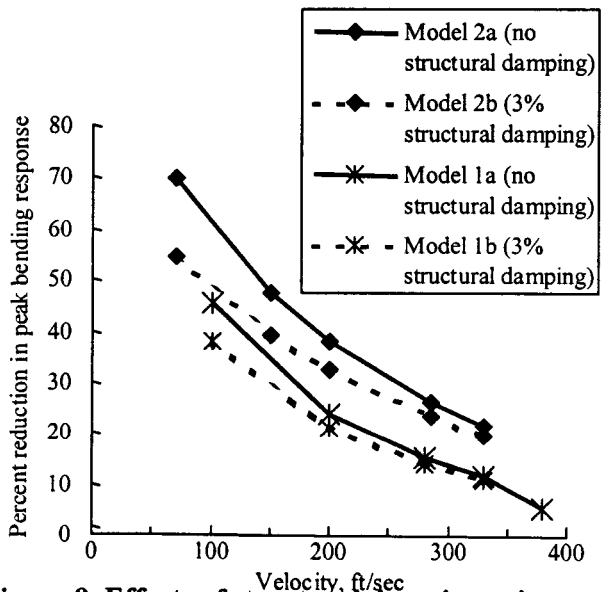


Figure 9. Effects of structural damping using models that are actively shunted

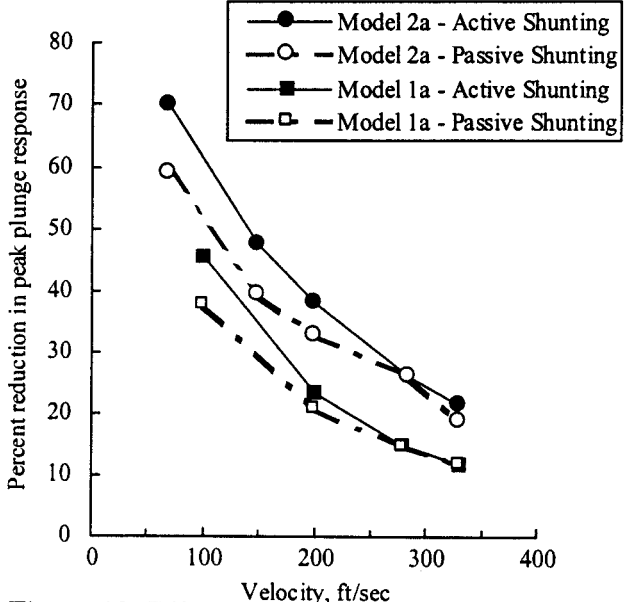


Figure 10. Effects of active versus passive shunting using models with no structural damping